Bioresource Technology 289 (2019) 121717

Contents lists available at ScienceDirect

Bioresource Technology

journal homepage: www.elsevier.com/locate/biortech

A two-stage model with nitrogen and silicon limitation enhances lipid productivity and biodiesel features of the marine bloom-forming diatom *Skeletonema costatum*

Guang Gao[a,b], Min Wu[a], Qianqian Fu[a], Xinshu Li[a], Juntian Xu[a,c,d,*]

[a] Jiangsu Key Laboratory of Marine Bioresources and Environment, Jiangsu Ocean University, Lianyungang 222005, China
[b] State Key Laboratory of Marine Environmental Science, Xiamen University, Xiamen 361005, China
[c] Co-Innovation Center of Jiangsu Marine Bio-industry Technology, Lianyungang 222005, China
[d] Jiangsu Key Laboratory of Marine Biotechnology, Jiangsu Ocean University, Lianyungang 222005, China

ARTICLE INFO

Keywords:
Biochemical
Biodiesel
Diatom
Lipid
Fatty acid
Photosynthesis

ABSTRACT

To enhance biodiesel production and quality from a bloom-forming diatom *Skeletonema costatum*, a two-stage model, in which cells were cultured in nutrient replete conditions first and then transferred to nutrient limitation conditions, was explored. Compared to one-stage model, nutrient limitation in the second stage significantly increased lipid content in spite of decreasing growth; consequently, Si-limitation and N-Si-limitation respectively increased lipid productivity by 37.6% and 76.7% for 6 h induction, and 42.8% and 113.7% for 12 induction. Nutrient limitation enhanced the proportions of saturated fatty acids (SFA) and monounsaturated fatty acids (MUFA) but reduced polyunsaturated fatty acid (PUFA). Therefore, N-Si-limitation reduced iodine value by 33.7% and 45.6% but increased cetane number by 6.4% and 21.6% for 6 and 24 h induction, respectively. These findings indicate that the two-stage model with N-Si-limitation can enhance lipid productivity as well as biodiesel quality from diatoms.

1. Introduction

Due mainly to the burning of fossil fuels, the atmosphere CO_2 level has been rising and increased by 46% since the industrial revolution. Increased CO_2 leads to global warming and global surface temperature by the end of the 21st century is likely to rise exceeding 2 °C for Representative Concentration Pathway (RCP) 6.0 and RCP8.5 (IPCC, 2013). Furthermore, the latest IPCC report provides clear scientific evidence that global warming is likely to reach 1.5 °C between 2030 and 2052 if it continues to increase at the current rate (IPCC SR1.5°C, 2018). The potential risks on extreme weather, species loss and extinction, food security and human health are much larger if global warming is 2.0 °C rather than 1.5 °C above the pre-industrial levels (IPCC SR1.5°C, 2018). With no or limited overshoot of 1.5 °C, global net anthropogenic CO_2 emissions must be reduced by about 45% by 2030 compared to the level in 2010 and reach net zero around 2050 (IPCC SR1.5°C, 2018).

To use carbon-zero fuels is an effective approach to reduce CO_2 emission and alleviate global warming. Among the various potential sources of renewable and carbon-zero energy, biofuels are of most interest and are expected to play an essential role in the global energy infrastructure and remitting global warming (Mishra et al., 2018). In comparison to other feedstocks, algae can provide a high-yield source of biofuels without competing arable land with crops and hence gain increasing attentions (Pandey et al., 2018). It is worth noting that although algal biofuel seems to be carbon-zero energy in theory all stages including cultivation, harvesting and post processing are energy-dependent. Therefore, it is difficult to conclude that biodiesel from microalgae is indeed environmentally benign when the whole cycle is considered, though algae absorb CO_2 when be cultivated. Various algae, including micro and macro, freshwater and seawater, have been tested for the use in biofuel (Adeniyi et al., 2018). Among them, green microalgae, including *Chlorella* and *Dunaliella*, have received much attention due to their advantage in growth and lipid content (Dickinson et al., 2017; Sakarika and Kornaros, 2019).

Diatoms are among the most productive and environmentally flexible eukaryotic microalgae on the planet. They are the dominant primary producers in the ocean contributing to approximately 20% of global carbon fixation (Nelson et al., 1995; Gao et al., 2018a). In addition, diatoms have a strong capacity in dealing with light and

* Corresponding author at: Jiangsu Key Laboratory of Marine Bioresources and Environment, Jiangsu Ocean University, Lianyungang 222005, China.
E-mail address: jtxu@hhit.edu.cn (J. Xu).

https://doi.org/10.1016/j.biortech.2019.121717
Received 29 May 2019; Received in revised form 25 June 2019; Accepted 26 June 2019
Available online 27 June 2019

temperature fluctuation (Gao et al., 2009; Souffreau et al., 2010; Gao et al., 2018a; Yuan et al., 2018), suggesting the potential for outdoor cultivation. However, compared to green microalgae, diatoms are not commonly considered for bio-oil production although some studies demonstrate the potential of diatoms in biofuel source (Hildebrand et al., 2012; Levitan et al., 2014). The reasons may be manifold and one of them is that diatoms commonly do not contain as much oil as green microalgae (Jiang et al., 2016; Shuba and Kifle, 2018).

Nitrogen-deficiency is proven to be an efficient approach to induce lipid accumulation in microalgae (Brennan and Owende, 2010; Jiang et al., 2016). In terms of diatoms, silicon-deficient has also been used to enhance lipid content (Smith et al., 2016). Although nitrogen or silicon-deficiency can induce more lipids, growth is dramatically reduced under such conditions, leading to lower lipid productivity (Jiang et al., 2016). Since the culture condition for lipid production differs from that required for cell growth, how to optimize culture conditions to obtain both fast growth rates and high lipid content is a long-standing challenge.

Accordingly, a two-stage culture system is proposed to resolve this problem, in which growth and lipid production are split into separate phases. This culture system has succeeded in *Nannochloropsis oculata* (Aléman-Nava et al., 2017) and *Chlorella* sp. (Nayak et al., 2019). However, the information regarding the use of this two-stage model on diatoms is very limited. Furthermore, *Skeletonema costatum*, a bloom-forming alga, has high growth rates when nutrient are replete and is resilient to pH fluctuation during bloom development (Gao et al., 2018b). In addition, it is a cosmopolitan species, common from tropical to polar climates, from fresh water through brackish to fully saline environments by virtue of its tolerance of a wide range of salinities and water temperatures. These characters endow it high tolerance against harsh operating conditions caused by variation of pH, temperature, or salinity, making it attractive in the use for biofuel based on the strain selection criteria (Dickinson et al., 2017). However, little is known on the potential of this alga in biofuel and how to improve lipid productivity and biodiesel features of this alga. Based on the previous studies (Aléman-Nava et al., 2017; Nayak et al., 2019), we proposed that the two-stage model with co-limitation of nitrogen and silicon may enhance lipid productivity and biodiesel quality of this alga. In this study, we cultured *S. costatum* in a two-stage model and analyzed lipid productivity, iodine value and cetane number, etc, to test this hypothesis and explore the potential of *S. costatum* in biodiesel application. Our study supplies solid contribution to use this bloom-forming alga in biofuel production.

2. Materials and methods

2.1. Species collection and culture conditions

Skeletonema costatum was isolated from coastal waters of the Yellow Sea (34°42′36.55″N, 119°29′24.37″E), Lianyungang City, Jiangsu Province, China. Cells were cultured with natural seawater enriched with F/2 medium in 1 L Erlenmeyer flasks containing 900 mL of media. Cultures were maintained at 20 °C and illuminated with cool white fluorescent tubes (200 μmol photons $m^{-2} s^{-1}$) with a 12 h:12 h light dark cycle. The culture was aerated and the air was filtered through a 0.22 μm filter (Milipore, America). The cells in exponential growth phase were taken for the following experiment.

2.2. Experimental design

In this experiment, a two-stage culture model was used to enhance the lipid productivity of *S. costatum*. In the first stage, cells were cultured semi-continuously in the nutrient replete condition as described above to obtain a high growth rate for five days. The initial cell density was 5×10^5 cells mL^{-1} and an average specific growth rate of $1.39 \pm 0.13\ d^{-1}$ was obtained during the first stage. In the second stage, cells were collected by centrifugation (5000 *g*, 10 min) and transferred to nutrient deficient conditions. The initial cell density was still 5×10^5 cells mL^{-1}. Three nutrient deficient conditions, N-limitation (6.8 μmol L^{-1}), Si-limitation (0.36 μmol L^{-1}) and N-Si-limitation (6.8 μmol L^{-1} for N and 0.36 μmol L^{-1} for Si), were set. The culture that was not transferred to nutrient limitation conditions was set as the control (889.2 μmol L^{-1} for N and 105.6 μmol L^{-1} for Si), representing the one-stage culture model. Induction was conducted for 6, 12 and 24 h. To obtain enough biomass for the following measurements, separate flasks were used for these three induction times. The experiment was conducted in triplicate.

2.3. Cell density and size determination

Two mL of algal solution was taken out at different induction periods, and the cell density was measured by the optical density at 680 nm (Doan et al., 2011) using a microplate reader (Thermo, Multiskan GO, America) with a standard curve. Meanwhile, 2 mL of algal solution was used to measure the cell size with a microscope (DM500, Leica, Germany).

2.4. Photosynthesis and respiration measurements

The net photosynthetic rate and respiration rate were determined by a Clark-type oxygen electrode (Hansatech, England). The light intensity and temperature were consistent with the growth conditions. Two mL of sample was transferred to an oxygen electrode tube with a rotor being continuously stirred during the measurement. The net photosynthetic and respiration rates (pmol O_2 $cell^{-1}$ h^{-1}) were determined by the changes of oxygen content in seawater within 5 min in light and darkness, respectively.

2.5. Determination of pigments

Fifty mL of sample was filtered onto a GF/F membrane (25 mm, Whatman) and placed in a refrigerator (4 °C) overnight in darkness after 5 mL of methanol was added. After centrifugation (5000 *g*, 10 min), the supernatant was measured by a microplate reader (Thermo, Multiskan GO, USA). The concentrations of chlorophyll *a* and carotenoid were calculated according to Gao et al. (2009).

2.6. Determination of biochemical composition

The soluble protein content of the algae was determined by the Bradford method (Bradford, 1976) and the soluble carbohydrate was determined by the Anthrone-Sulphuric Acid Colorimetric method (Deriaz, 1961).

Total lipid extraction was conducted according to the modified Folch method (Folch et al., 1957). The algal cells were collected by centrifugation (7500 *g*, 5 min) and dried in an oven at 60 °C to constant weight. Fifty mg of algae powder was grinded, transferred to a 10 mL centrifuge tube, and then 5 mL chloroform methanol mixture (V:V = 2:1) and 1 mL NaCl (0.88%) solution were added. After being shaken on a multi-tube vortex mixer (DMT-2500, China) for 20 min (2000 rpm), the solution was centrifuged (5000 *g*, 5 min) and the supernatant was removed. Then 5 mL of methanol-water solution mixed solution (V:V = 1:1) was added to the centrifuge tube. After centrifuging and removing the upper phase once more, the bottom phase was dried under a steady stream of nitrogen supplied by a nitrogen blowing instrument (Autoscience MTN-5800, China). Lipid content (pg $cell^{-1}$/% dry weight (DW)) was calculated based on the lipid weight and cell number/weight. Lipid productivity (mg L^{-1}) was determined by the changes of lipid production during the induction periods (6, 12 and 24 h).

The fatty acids were converted to fatty acid methyl esters (FAMEs) by H_2SO_4-CH_3OH (2.0%, v/v) method. About 20 mg of algal flour and

2 mL of H_2SO_4-CH_3OH were placed in a centrifuge tube, mixed with a multi-tube vortex mixer (DMT-2500, China) for 10 min, and heated in water bath at 80 °C for 1 h. Then 1 mL of deionized water and 2 mL of isooctane were added and the mixture was centrifuged at 1700 *g* for 5 min. The supernatant layer containing FAMEs was taken, and filtered through a filter (0.22 μm, Leigu, China) and analyzed by a gas chromatography mass spectrometer (Shimadzu, GCMS-QP2010SE, Japan). The 20 μL injection was analyzed using an Agilent DB-23 (60 m × 0.25 mm × 0.25 μm film thickness) polar stationary phase column. Purified helium was used as a carrier gas with a head pressure of 150.0 kPa and a column flow of 0.17 mL min^{-1}. The inlet and detector temperature was 250 °C and 200 °C, respectively. The temperature program was as follows: the initial temperature was 50 °C for 4 min; then it was raised to 175 °C at a rate of 25 °C min^{-1}, and then increased to 230 °C at a rate of 4 °C min^{-1} for 5 min. Chromatograph peaks were identified according to the retention time of a Supelco 37 component FAME mix (Sigma-Aldrich). Quantification of FA was based on peak areas of individual peaks identified, expressed as a percentage of the total peak areas for total FA. All samplings were conducted in triplicate.

2.7. Quality properties of biodiesel

Physical characteristics of fatty acids were determined by number of double bond, chain length and proportion of each fatty ester components in total fatty acids. The quality of biodiesel was assessed by determining the saponification value (SV), iodine value (IV), cetane number (CN) using relations shown in Eqs. (1)–(3) (Francisco et al., 2010),

$$SV = \sum (560 \times A_i)/MW_i \quad (1)$$

$$IV = \sum (254 \times m \times A_i)/MW_i \quad (2)$$

$$CN = 46.3 + 5458/SV - 0.225 \times IV \quad (3)$$

where A_i is the percentage of each fatty acid, MW_i is the molecular mass of each fatty acid, and m is the number of double bond.

2.8. Statistical analysis

Data analysis was performed using SPSS v.21 and the data was expressed as means ± standard deviation (SD). The data under every treatment conformed to a normal distribution (Shapiro-Wilk, $P > 0.05$) and the variances could be considered equal (Levene's test, $P > 0.05$). Considering that cells during different induction periods were from separate flasks, two-way analysis of variance (ANOVA) rather than repeated-measures ANOVA was conducted to analyze the effects of nutrient limitation and induction time on cell density, cell diameter, net photosynthetic rate, respiration rate, Chl *a* content, carotenoid content, soluble protein, soluble carbohydrate, lipid content, lipid productivity, iodine value and cetane number. Two-way multivariate analysis of variance (MANOVA) was conducted to assess the effects of nutrient limitation and induction time on fatty acids. Least significant difference was used to for *post hoc* analysis. *P*-values less than 0.05 were considered as statistically significant. The statistical outcome can be found in the Supplementary file.

3. Results and discussion

3.1. Growth and biochemical composition

The changes of cell density after transferred to nutrient limitation conditions were first recorded (Fig. 1a). Two-way ANOVA showed that both nutrient limitation and induction time affected cell density, and they had an interactive effect. After 6 h induction, cell density was reduced by N-limitation, with further decrease under the N-Si-limitation,

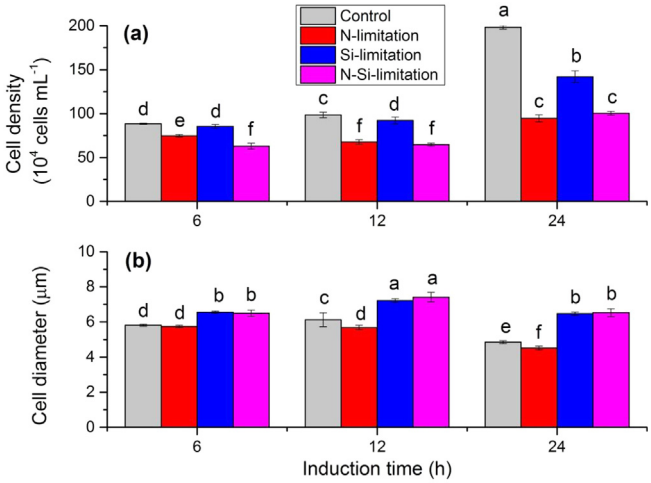

Fig. 1. Changes of cell density (a) and cell diameter (b) in *S. costatum* under different nutrient treatments over the induction period. The initial cell density was 5×10^5 cells mL^{-1}. The culture that was not transferred to nutrient limitation conditions was set as control, representing the one-stage culture model. Significant differences ($P < 0.05$) among the treatments are indicated by different lowercase letters (n = 3).

while Si-limitation alone did not have a significant effect. By 12 h induction, both N-limitation and Si-limitation reduced cell density although N-limitation led to larger decrease. Compared to N-limitation, N-Si-limitation did not lead to further decrease. The trend of 24 h induction was similar to 12 h although the inhibitory effect of nutrient limitation exacerbated further. In terms of the effect of induction time, cell density increased with induction time for the control whereas it did not increase for those under nutrient limitation when induction time changed from 6 h to 12 h.

Apart from cell density, the changes of cell size under various treatments were also investigated (Fig. 1b). Both nutrient limitation and induction time affect cell diameter and they had an interactive effect. After 6 h induction, N-limitation did not affect cell diameter but Si-limitation and N-Si-limitation increased it. After 12 h induction, N-limitation led to a slight decrease in cell diameter while Si-limitation and N-Si-limitation still increased it. A similar pattern was found in 24 h induction. With the extend of induction time, cell size increased first and then decreased for all nutrient limitation treatments although the change for N-limitation between 6 and 12 h was not statistically significant.

Induction time and nutrient limitation also interacted on net photosynthetic rate, with each having a significant effect (Fig. 2a). After 6 h induction, N-limitation decreased net photosynthetic rate while neither Si-limitation nor N-Si-limitation affected it. After 12 h induction, N-limitation or Si-limitation did not affect net photosynthetic rate, while N-Si-limitation resulted in a significant increase. At the end of 24 h induction, N-limitation increased net photosynthetic rate, with insignificant effects from Si-limitation and N-Si-limitation. The effect of induction time on net photosynthetic rate depended on nutrient limitation. The net photosynthetic rate for control and Si-limitation did not change and then decreased when induction time increased from 6 h to 12 h and then to 24 h, while the pattern was first increase and then nonchange for N-limitation and first increase and then decrease for N-Si-limitation.

In terms of respiration rate, both nutrient limitation and induction time had a significant effect on it, and these two factors had a noticeable interactive effect (Fig. 2b). After 6 h induction, neither N-limitation nor Si-limitation significantly affected respiration rate but N-Si-limitation decreased it compared to the control. After 12 h induction, N-limitation increased respiration rate and N-Si-limitation resulted in a further increase, while Si-limitation alone did not affect it. By 24 h

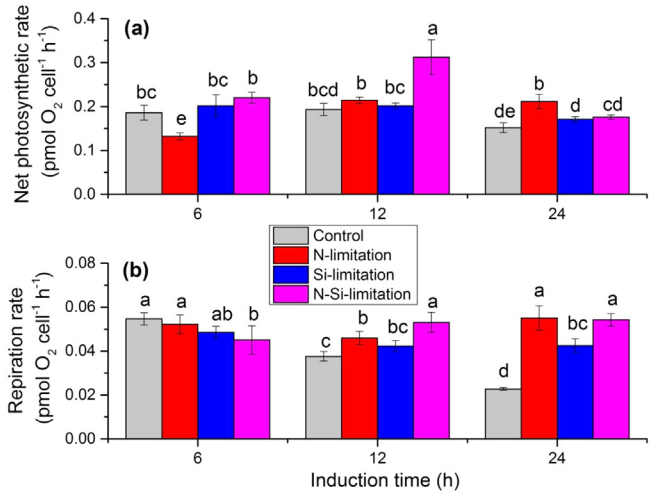

Fig. 2. Changes of net photosynthetic rate (a) and respiration rate (b) in *S. costatum* under different nutrient treatments over the induction period. The culture that was not transferred to nutrient limitation conditions was set as control, representing the one-stage culture model. Significant differences ($P < 0.05$) among the treatments are indicated by different lowercase letters (n = 3).

induction, each treatment led to remarkable increase in respiration rate, with least effect found under Si-limitation. The respiration rate under the control condition dramatically decreased with induction time, while the changes were not significant or slightly significant under nutrient limitation conditions.

In terms of photosynthetic pigment, nutrient limitation and induction time interacted on Chl *a* content, with each having a significant effect (Fig. 3a). After 6 h induction, Si-limitation and N-Si-limitation significantly increased Chl *a* content, with neutral effect of N-limitation. After 12 h induction, no treatment altered Chl *a* content. After 24 h induction, N-limitation reduced Chl *a* content, Si-limitation increased it while N-Si-limitation did not affect it. With the extension of induction time, Chl *a* content under N-limitation did not vary while it first decreased and then increased under the other treatments.

In addition to Chl *a*, Nutrient limitation and induction time also interacted on another photosynthetic pigment, carotenoid (Fig. 3b). After 6 h induction, N-limitation did not change carotenoid content significantly while both Si-limitation and N-Si-limitation enhanced it.

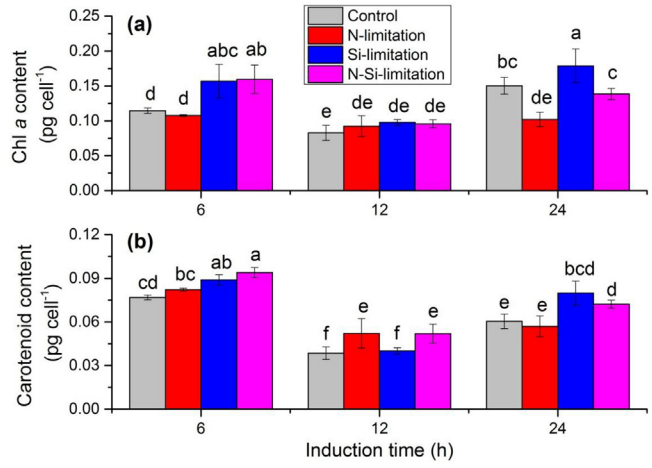

Fig. 3. . Changes of Chl *a* (a) and carotenoid (b) in *S. costatum* under different nutrient treatments over the induction period. The culture that was not transferred to nutrient limitation conditions was set as control, representing the one-stage culture model. Significant differences ($P < 0.05$) among the treatments are indicated by different lowercase letters (n = 3).

After 12 h induction, both N-limitation and N-Si-limitation increased carotenoid content, with neutral effect of Si-limitation. After 24 h induction, N-limitation did not change carotenoid content while Si-limitation and N-Si-limitation increased it. When induction time changed from 6 h to 24 h, carotenoid content under all treatments decreased largely and then increased slightly although the increase for N-limitation was not statistically significant.

Two-way ANOVA showed that nutrient limitation and induction time interacted on the synthesis of soluble protein, with each having a significant effect (Fig. 4a & b). For soluble protein per cell (Fig. 4a), after 6 h induction, any nutrient limitation did not affect it; after 12 h induction, Si-limitation did not affect it while both N-limitation and N-Si-limitation resulted in a significant decrease; at the end of 24 h induction, N-limitation and N-Si-limitation significantly reduced it while Si-limitation still did not affect it. With the increase of induction time, the soluble protein content per cell under control and Si-limitation increased first and then decreased, while it continuously decreased under N-limitation and N-Si-limitation. For soluble protein content of DW (Fig. 4b), after 6 h incubation, N-limitation increased it but Si-limitation and N-Si-limitation decreased it; after 12 h incubation, N-limitation did not affect it while Si-limitation and N-Si-limitation decreased it; the pattern of 24 h incubation was the same as 12 h. With the increase of induction time, the soluble protein content of DW did not change under control but generally decreased for nutrient-limitation conditions.

Nutrient limitation and induction time also interacted on the content of soluble carbohydrate, with each having a significant effect (Fig. 4c & d). For soluble carbohydrate content per cell (Fig. 4c), after 6 h induction, N-limitation significantly increased it, N-Si-limitation resulted in a further increase while Si-limitation reduced it; after 12 h induction, all treatments increased it, with largest effect from N-Si-limitation and smallest from Si-limitation; at the end of 24 h induction, Si-limitation did not affect it while both N-limitation and N-Si-limitation led to a dramatic increase. The content of soluble carbohydrate per cell under control decreased with induction time while it had a rising trend under N-limitation. For soluble carbohydrate content of DW (Fig. 4d), after 6 h induction, N-limitation increased it while Si-limitation reduced it; after 12 h induction, both N-limitation and N-Si-limitation increased it; at the end of 24 h induction, both N-limitation and N-Si-limitation increased it but Si-limitation decreased it. With the extension of induction time, soluble carbohydrate content of DW decreased under control and Si-limitation but increased under N-limitation and N-Si-limitation. Nitrogen is an indispensable element for all plants in terms of the biosynthesis of macromolecules, such as proteins, nucleic acids, and chlorophyll (Gao et al., 2018c). The previous studies show the importance of nitrogen on growth of *S. costatum* (Liu et al., 2012; Gao et al., 2018b). Nitrate limitation dramatically decreased growth of *S. costatum* in this study. *S. costatum* is considered as an opportunist, which can grow fast and form bloom when nutrients are replete. Our study confirm that the essential role of nitrate on growth of *S. costatum*. However, nitrogen limitation did not reduce net photosynthetic rate or content of photosynthetic pigment at most cases, showing the strong photosynthetic capacity of *S. costatum* to deal with environmental stress. The energy generated from photosynthesis was not used for cell division but flowed to the synthesis of carbohydrate and lipid, which led to increased content of carbohydrate and lipid. It seems that *S. costatum* acclimates to environmental changes by reorganising energy allocation and utilization in spite of the sacrifice of growth. The enhanced reparation rate under N limitation and N-Si limitation also supported the hypothesis that metabolic activities were enhanced to maintain intracellular homeostasis under environmental stress.

Silicon is also needed for a large amount of organisms, from unicellular algae to vascular plants, to produce siliceous structures, referring to external and internal skeletons (Knight et al., 2016). Silicon is particularly important for diatom as the cell walls of diatoms are silicified, forming a unique structure termed frustule. Consequently,

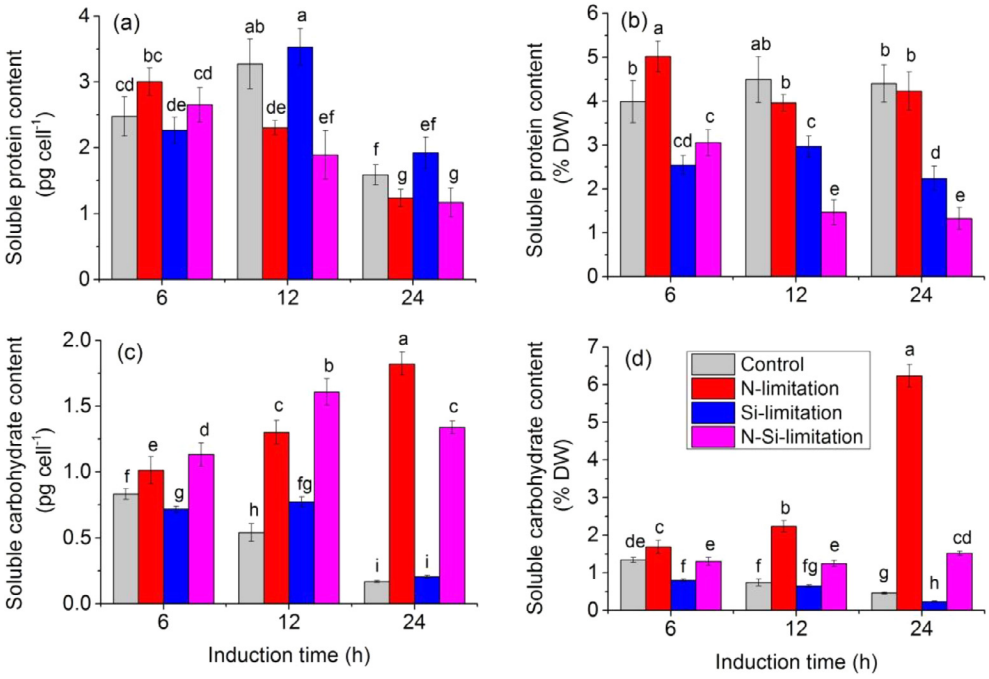

Fig. 4. Content changes of soluble protein (a, b) and carbohydrate (c, d) in *S. costatum* under different nutrient treatments over the induction period. The culture that was not transferred to nutrient limitation conditions was set as control, representing the one-stage culture model. Significant differences ($P < 0.05$) among the treatments are indicated by different lowercase letters (n = 3).

silicon availability affects morphology, motility and growth of diatoms (Bondoc et al., 2016; Leynaert et al., 2018). However, silicon limitation did not significantly affect growth of *S. costatum* in this study. It has reported that diatom can decrease silica content in cells to avoid growth limitation (McNair et al., 2018). This may also occur in *S. costatum*. It seems that nitrogen plays a more significant role in growth of *S. costatum* compared to silicon and nitrogen limitation can cover the effect of silicon limitation.

3.2. Lipid production

Both induction time and nutrient limitation affected lipid content (Fig. 5a & b). For lipid content per cell (Fig. 5a), after 6 h induction, N-limitation and Si-limitation resulted in similar increases while a more remarkable increase was induced by N-Si-limitation; a similar pattern was found at 12 h induction; at the end of 24 h induction, although N-limitation and Si-limitation still stimulated synthesis of lipid, the N-Si-limitation did not induce lipidsynthesis further. Lipid content per cell under the control, N-limitation or Si-limitation did not change when induction time went from 6 h to 12 h but decreased at 24 h induction. Under N-Si-limitation, lipid content first increased and then decreased, making the highest value occur at 12 h induction. For lipid content of DW (Fig. 5b), after 6 h induction, N-limitation and N-Si-limitation increased it; a similar pattern was found at 12 h induction; at the end of

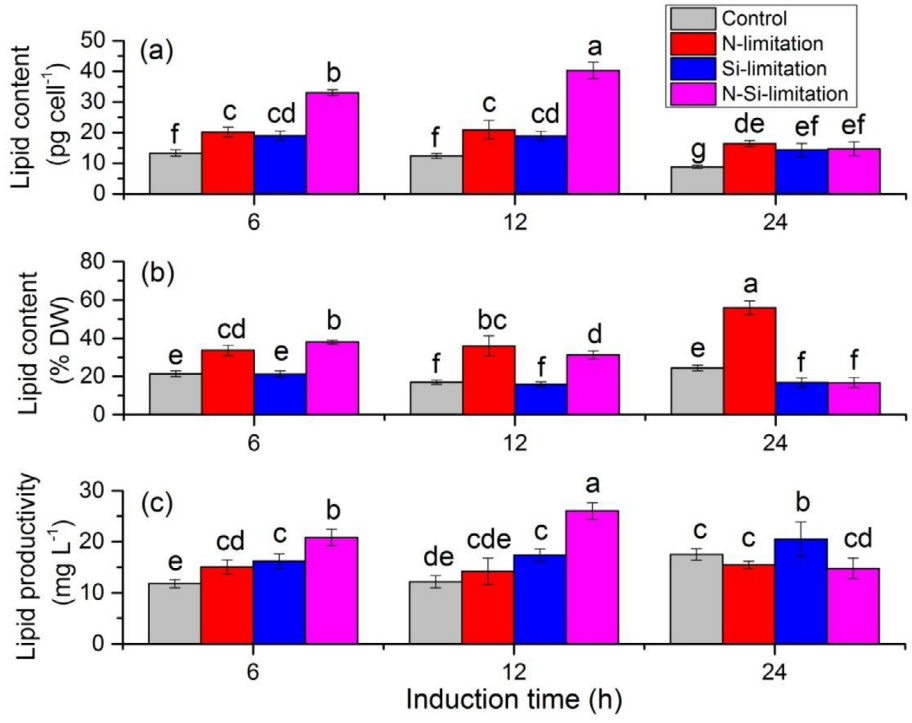

Fig. 5. Changes of lipid content (a, b) and productivity (c) in *S. costatum* under different nutrient treatments over the induction period. The culture that was not transferred to nutrient limitation conditions was set as control, representing the one-stage culture model. Significant differences ($P < 0.05$) among the treatments are indicated by different lowercase letters (n = 3).

24 h induction, N-limitation dramatically stimulated it while both Si-limitation and N-Si-limitation led to decreases.

Nitrogen is found to be a critical factor that affects lipid content in algae and nitrogen limitation is commonly used to stimulate lipid accumulation in microalgae for biofuel or health care product (Brennan and Owende, 2010; Fields et al., 2014; Sibi et al., 2016). Generally, there are two hypotheses for the stimulatory effect of nitrogen limitation on lipid accumulation. One is that nitrogen deficiency almost invariably causes a steady decline in cell division rate; at the same time, biosynthesis of fatty acids can continue under such conditions. This thereby results in increased lipid content per cell (Brennan and Owende, 2010; Gao et al., 2018c). The other hypothesis is that when nitrogen is scarce, protein synthesis is suspended and the flow of intracellular carbon is diverted from protein to either lipid or carbohydrate synthesis (Gao et al., 2018c). Compared to carbohydrates, triacylglycerides composed primarily of saturated and monounsaturated fatty acids are more energy-effective and thus preferentially synthesized for rebuilding the cell after the stress (Rodolfi et al., 2009; Gao et al., 2018c). Lipid content was enhanced by nitrogen limitation in this study and the size of cells under nitrogen limitation was not enhanced compared to the control, which denies the first hypothesis. Meanwhile, decreased protein content per cell was found under the nitrogen limitation condition after 12 and 24 h incubation, indicating that carbon and energy were transferred from protein to lipid synthesis and supporting the second hypothesis. In summary, it seems that the stimulatory effect of nitrogen limitation on lipid content was due to more carbon skeleton and energy flowed from protein synthesis to lipid synthesis rather than the enlarged cell size. The lipid content of *S. costatum* growing under control ranged from 17.0 to 24.4%DW, which was similar to Rekha et al (2012)'s result on *S. costatum* (21.6%). The highest lipid content was 56.0% at N-limitation of 24 h induction, which is higher than most other algal strains (Griffiths and Harrison, 2009).

In addition to nitrogen, silicon limitation also induced lipid accumulation in *S. costatum* in this study. In contrast to nitrogen limitation, silicon limitation did not affect protein content, but significantly enhanced cell size, indicating that the mechanisms of stimulating lipid accumulation in *S. costatum* are different between nitrogen and silicon limitation. In contrast to nitrogen starvation, silicon starvation is considered to have less effect on overall metabolic activities, making it a unique approach to induce lipid accumulation with little other detrimental effect on cellular function (Smith et al., 2016; Shrestha and Hildebrand, 2017). This is confirmed by the present study as silicon limitation did not change the content of protein or carbohydrate in *S. costatum* as much as nitrogen limitation.

Furthermore, the combination of nitrogen and silicon limitation further increased lipid synthesis. A similar finding was reported in a freshwater diatom, RGd-1 (Moll et al., 2014). The potential mechanisms for the addictive effect of nitrogen and silicon can be explained by the combination of hypotheses one and two mentioned above. Specifically, the increased lipid content can be due to the combination of decreased cell division rate and increased carbon flow to lipid synthesis because cell size was largest and protein content was lowest under the combination of N and Si limitation.

In terms of lipid productivity, both nutrient limitation and induction time affected it (Fig. 5b). After 6 h induction, N-limitation and Si-limitation enhanced lipid productivity by 27.8% and 37.6%, respectively, and N-Si-limitation led to the largest increase of 76.7%. After 12 h induction, N-limitation did not change lipid productivity significantly but Si-limitation and N-Si-limitation increased it by 42.8% and 113.7%, respectively. After 24 h induction, only Si-limitation enhanced lipid productivity while N-limitation or N-Si-limitation did not have significant effects. Lipid productivity under control did not change with the induction time increasing from 6 h to 12 h, but increased after 24 h induction. A similar pattern was found under Si-limitation condition. Lipid productivity under N-limitation did not change over 24 h induction. The highest lipid productivity under N-Si-limitation occurred at 12 h induction, followed by 6 h. It seems that N-Si-limitation after 12 h induction was the optimal condition for lipid productivity of *S. costatum*.

Lipid productivity is considered as an essential index for biodiesel production (Griffiths and Harrison, 2009; Abu-Ghosh et al., 2018). Although nutrient limitation decreased growth rate of *S. costatum* in this study, they induced more lipid synthesis and thus resulted in higher lipid productivity. During the induction period, highest lipid productivity occurred under the N-Si-limitation at 12 h induction, which was 2.14 folds higher than the control and suggests the success of two-stage model in stimulating lipid productivity. This lipid productivity ($26.0 \pm 1.7\ mg\ L^{-1}$) is medium compared to other algal strains (Griffiths and Harrison, 2009). However, this productivity was based on 12 h rather than 24 h; it can lead most algal species if half of the culture time is considered (Griffiths and Harrison, 2009).

3.3. Biodiesel properties

The composition of fatty acids was also analyzed as it can determine the quality of biodiesel. Two-way MANOVA showed that nutrient limitation and induction time affected profile of fatty acids (Table 1). Nutrient limitation changed the proportions of all the fatty acids except c18:0, induction time affected the proportions of all the fatty acids except c15:0, nutrient limitation and induction time interacted on all the fatty acids except c18:0. Generally, N limitation did not affect saturated fatty acids (SFA) while Si-limitation and N-Si-limitation increased it by 3.6% and 3.8% respectively after 6 h induction (Table 1). After 12 h induction, the case was conversed; N limitation increased SFA by 2.9% but Si-limitation and N-Si-limitation did not affect it. After 24 h induction, all nutrient-limitation treatments increased SFA, with highest induction (14.2%) occurring at N-Si-limitation. In terms of monounsaturated fatty acids (MUFA), it was enhanced by each nutrient limitation at each induction time although the increase for N-limitation and Si-limitation at 12 h induction was not statistically significant. Contrast to SFA and MUFA, nutrient limitation reduced the proportion of polyunsaturated fatty acids (PUFA). For instance, Si-limitation and N-Si-limitation reduced it by 51.6% and 52.3% respectively compared to the control after 6 h induction; N-limitation and N-Si-limitation reduced it by 12.8% and 14.0% respectively compared to the control after 12 h induction; N-limitation, Si-limitation and N-Si-limitation reduced it by 49.9%, 39.4% and 55.7% respectively compared to the control after 24 h induction.

N limitation also increased proportion of SFA and MUFA, and reduce PUFA in *Skeletonema menzelii* SM-2 (Jiang et al., 2016) and *Phaeodactylum tricornutum* (Yang et al., 2013). Si limitation also increased proportion of SFA and MUFA, and reduce PUFA in the diatom *Cyclotella cryptica* (Roessler, 1988). Combined our findings with previous studies, it seems that algae commonly increase SFA and MUFA but reduce PUFA under nutrient limitation conditions. Yang et al (2013) found that transcript abundance of the fatty acid desaturase that is involved in MUFA synthesis increased whereas the expression of two desaturases catalyzing PUFA formation decreased under N deprivation, which may display the molecular mechanism of the changes in FA composition. From the perspective of physiological and ecological function, SFA and MUFA can store more energy compared to PUFA with same chain length. Therefore cells prefer to synthesize SFA or MUFA rather than PUFA under environmental stress, so that they can obtain more energy from SFA and MUFA to maintain hemostasis.

Long chain SFA and MUFA are suitable components for biodiesel because they improve oxidative stability without affecting the cold flow properties of biodiesel. On the other side, PUFA has a negative effect on oxidative stability of biodiesel as bisallylic hydrogens are susceptible for free radical attack, although it can enhance cold flow performance of biodiesel (Cho et al., 2016; Chandra et al., 2019). According to European standards EN14214, the percentages of linolenic acid (C18:3)

Table 1
Fatty acid composition of *S. costatum* under different nutrient treatments over the induction period (% of total FAME). Values are means of three replicates ± standard deviation. The culture that was not transferred to nutrient limitation conditions was set as control, representing the one-stage culture model. Significant differences ($P < 0.05$) among the treatments are indicated by different lowercase letters (n = 3). SFA, saturated fatty acids; MUFA, monounsaturated fatty acids; PUFA, polyunsaturated fatty acids.

Fatty acid		c12:0	c14:0	c15:0	c16:0	c16:1	c18:0	c18:1n-9c	c18:2n-6c
6 h induction	Control	0.12 ± 0.00^{c}	20.07 ± 0.22^{d}	1.24 ± 0.02^{c}	44.89 ± 0.25^{b}	16.55 ± 0.20^{e}	7.02 ± 0.39^{a}	0.22 ± 0.01^{cd}	0.28 ± 0.02^{e}
	N^-	0.09 ± 0.00^{c}	19.90 ± 0.48^{d}	1.08 ± 0.04^{e}	45.81 ± 0.42^{ab}	17.51 ± 0.35^{d}	6.29 ± 0.75^{a}	0.23 ± 0.00^{c}	0.35 ± 0.01^{d}
	Si^-	0.09 ± 0.00^{c}	23.11 ± 0.38^{c}	1.43 ± 0.02^{b}	45.33 ± 0.13^{b}	19.02 ± 0.08^{bc}	6.01 ± 0.11^{a}	0.22 ± 0.01^{cd}	0.23 ± 0.01^{f}
	N^-&Si^-	0.10 ± 0.01^{c}	23.43 ± 0.10^{c}	1.46 ± 0.01^{a}	45.16 ± 0.10^{b}	18.94 ± 0.02^{c}	5.96 ± 0.03^{a}	0.22 ± 0.00^{cd}	0.23 ± 0.00^{f}
12 h induction	Control	0.23 ± 0.09^{b}	17.74 ± 0.36^{e}	1.48 ± 0.02^{a}	45.36 ± 0.76^{ab}	19.39 ± 0.69^{ab}	4.38 ± 0.51^{b}	0.15 ± 0.04^{cde}	0.23 ± 0.01^{f}
	N^-	0.38 ± 0.08^{a}	16.73 ± 0.39^{e}	1.23 ± 0.03^{c}	48.11 ± 0.51^{a}	18.97 ± 0.28^{c}	4.71 ± 0.43^{b}	0.05 ± 0.02^{e}	0.37 ± 0.01^{d}
	Si^-	0.12 ± 0.05^{c}	17.26 ± 0.77^{e}	1.46 ± 0.06^{a}	45.93 ± 1.08^{ab}	19.68 ± 0.75^{ab}	4.03 ± 0.98^{bc}	0.13 ± 0.02^{de}	0.25 ± 0.02^{f}
	N^-&Si^-	0.13 ± 0.02^{c}	16.80 ± 1.01^{e}	1.16 ± 0.04^{d}	48.03 ± 1.21^{ab}	20.32 ± 0.66^{a}	3.65 ± 0.80^{bc}	0.22 ± 0.01^{c}	0.44 ± 0.01^{c}
24 h induction	Control	0.10 ± 0.01^{c}	31.79 ± 2.34^{a}	1.51 ± 0.01^{a}	25.64 ± 3.17e	14.78 ± 0.53^{f}	3.25 ± 1.25^{c}	0.07 ± 0.02^{de}	0.57 ± 0.02^{a}
	N^-	0.24 ± 0.15^{b}	26.64 ± 0.87^{b}	1.20 ± 0.06^{cd}	38.91 ± 1.08^{d}	18.54 ± 0.70^{c}	2.59 ± 0.52^{cd}	0.42 ± 0.31^{b}	0.51 ± 0.06^{b}
	Si^-	0.11 ± 0.02^{c}	27.19 ± 2.57^{b}	1.44 ± 0.04^{b}	36.08 ± 3.90^{d}	19.30 ± 0.94^{b}	1.93 ± 1.22^{d}	0.07 ± 0.03^{de}	0.36 ± 0.01^{d}
	N^-&Si^-	0.10 ± 0.02^{c}	24.52 ± 0.97^{c}	1.08 ± 0.02^{e}	42.10 ± 1.45^{c}	18.10 ± 0.51^{cd}	3.31 ± 0.74^{c}	0.66 ± 0.01^{a}	0.42 ± 0.01^{c}

Fatty acid		c18:3n-6	c18:3n-3	c20:4n-6	c20:5n-3	c22:6n-3	SFA	MUFA	PUFA
6 h induction	Control	0.06 ± 0.01^{fg}	0.14 ± 0.01^{e}	0.04 ± 0.00^{g}	7.95 ± 0.27^{cd}	1.41 ± 0.08^{def}	73.34 ± 0.48^{b}	16.77 ± 0.20^{e}	9.89 ± 0.36^{de}
	N^-	0.08 ± 0.01^{ef}	0.17 ± 0.01^{cd}	0.04 ± 0.01^{fg}	7.20 ± 0.25^{d}	1.26 ± 0.02^{f}	73.18 ± 0.66^{bc}	17.74 ± 0.36^{d}	9.08 ± 0.30^{e}
	Si^-	0.05 ± 0.01^{g}	0.11 ± 0.00^{f}	0.02 ± 0.00^{h}	3.95 ± 0.08^{e}	0.45 ± 0.01^{g}	75.97 ± 0.17^{a}	19.24 ± 0.09^{bc}	4.79 ± 0.08^{f}
	N^-&Si^-	0.05 ± 0.01^{g}	0.11 ± 0.00^{f}	0.02 ± 0.01^{h}	3.88 ± 0.01^{e}	0.43 ± 0.01^{g}	76.11 ± 0.04^{a}	19.16 ± 0.03^{bc}	4.72 ± 0.01^{f}
12 h induction	Control	0.09 ± 0.01^{de}	0.11 ± 0.00^{f}	0.07 ± 0.00^{ef}	8.87 ± 0.30^{c}	1.91 ± 0.10^{bc}	69.18 ± 0.90^{de}	19.55 ± 0.68^{bc}	11.27 ± 0.38^{cd}
	N^-	0.11 ± 0.00^{d}	0.16 ± 0.01^{d}	0.08 ± 0.01^{de}	7.59 ± 0.28^{d}	1.52 ± 0.05^{d}	71.16 ± 0.64^{bc}	19.02 ± 0.29^{bc}	9.83 ± 0.35^{e}
	Si^-	0.08 ± 0.00^{ef}	0.11 ± 0.01^{f}	0.06 ± 0.00e	9.05 ± 0.70^{c}	1.86 ± 0.13^{c}	68.79 ± 1.59^{ef}	19.81 ± 0.73^{ab}	11.41 ± 0.86^{c}
	N^-&Si^-	0.13 ± 0.01^{c}	0.17 ± 0.01^{bcd}	0.08 ± 0.00^{d}	7.42 ± 0.36^{d}	1.45 ± 0.07^{de}	69.77 ± 0.94^{de}	20.54 ± 0.65^{a}	9.66 ± 0.48^{e}
24 h induction	Control	0.09 ± 0.01^{de}	0.21 ± 0.02^{a}	0.12 ± 0.01^{c}	18.57 ± 1.70^{a}	3.33 ± 0.22^{a}	62.28 ± 2.41^{g}	14.84 ± 0.51^{f}	22.88 ± 1.92^{a}
	N^-	0.21 ± 0.01^{a}	0.22 ± 0.01^{a}	0.18 ± 0.01^{a}	8.88 ± 0.33^{c}	1.46 ± 0.03^{de}	69.58 ± 0.88^{de}	18.96 ± 0.56^{bc}	11.46 ± 0.33^{c}
	Si^-	0.18 ± 0.03^{b}	0.11 ± 0.01^{f}	0.09 ± 0.01^{d}	11.09 ± 1.66^{b}	2.05 ± 0.11^{b}	66.75 ± 2.62^{f}	19.37 ± 0.91^{b}	13.87 ± 1.80^{b}
	N^-&Si^-	0.20 ± 0.02^{ab}	0.18 ± 0.00^{b}	0.16 ± 0.01^{b}	7.87 ± 0.59^{c}	1.31 ± 0.10^{ef}	71.10 ± 1.17^{cd}	18.76 ± 0.51^{c}	10.14 ± 0.71^{cde}

and stearidonic acid (C18:4) must be under 12% and 1%, respectively, for an ideal biodiesel (Gouveia et al., 2009; Pereira et al., 2013). In this study, the percentages of linolenic acid under various culture conditions were below 0.3% and stearidonic acid was undetectable.

Based on the composition of fatty acids, two important parameters (iodine value and cetane number) indicating biodiesel quality were calculated. Both nutrient limitation and induction time affected iodine value and they had an interactive effect (Fig. 6a). After 6 h induction, N-limitation did not affect iodine value but Si-limitation and N-Si-limitation significantly reduced it by 33.0% and 33.7%, respectively. After 12 h induction, N-limitation and N-Si-limitation reduced iodine value by 10.8% and 9.8% respectively while Si-limitation did not have a significant effect. After 24 h induction, each nutrient limitation reduced iodine value dramatically, with largest decrease (45.6%) under N-Si-limitation, followed by N-limitation (40.6%). With the increase of induction time, iodine value under each treatment increased although some changes for N-limitation and N-Si-limitation were not statistically significant.

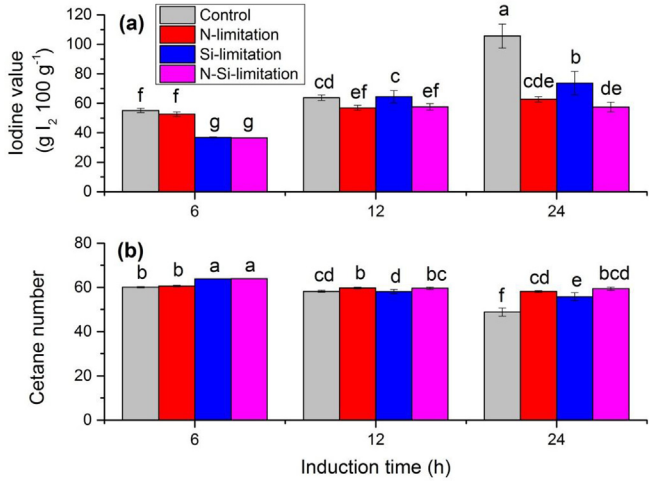

Fig. 6. Changes of iodine value (a) and cetane number (b) in *S. costatum* under different nutrient treatments over the induction period. The culture that was not transferred to nutrient limitation conditions was set as control, representing the one-stage culture model. Significant differences ($P < 0.05$) among the treatments are indicated by different lowercase letters (n = 3).

Nutrient limitation and induction time also interacted on cetane number, with each having a significant effect (Fig. 6b). After 6 h induction, N-limitation did not affect cetane number but Si-limitation and N-Si-limitation increased it by 6.3% and 6.4%, respectively. After 12 h induction, N-limitation increased cetane number by 2.6% while the effects of Si-limitation and N-Si-limitation were insignificant. After 24 h induction, each nutrient treatment increased cetane number, with smallest increase (14.2%) under Si-limitation and largest (21.6%) under N-Si-limitation. With the extension of induction time, cetane number under each treatment decreased although the changes between 6 and 12 h for N-limitation and between 12 and 24 h for N-Si-limitation were not statistically significant.

The iodine value (IV) represents the degree of unsaturation of biodiesel. More MUFA and PUFA can result in higher IV for biodiesel. Higher IV of the biodiesel can lead to polymerization of glycerides and deposition or deterioration of lubricant in the engine (Francisco et al., 2010; Aslam et al., 2018). Therefore, a lower IV is desirable for biodiesel. The European standard (EN 14214) defines a maximum value of 120 g I_2 100 g^{-1} (Francisco et al., 2010; Aslam et al., 2018). The IVs in this study were below 75 g I_2 100 g^{-1} except for higher value of 106 g I_2 100 g^{-1} under the control after 24 h induction. This indicates that IV of biodiesel from *S. costatum* conforms to the European standard. Cetane number is a dimensionless descriptor linked to fuel ignition quality in the diesel engine and higher cetane values indicate better combustion, less knocking, lower nitrous oxide emission and easier startup of engine

(Knothe, 2009, 2012; Cho et al., 2016). The minimum CN value of US standard (ASTM D6751), European (EN 14214) and Australian standard and National Petroleum Agency (ANP255) in Brazil are 47, 51, 51, and 45, respectively (Francisco et al., 2010; Aslam et al., 2018). The cetane numbers in the present study were all above 55 except for a lower value of 49 under the control after 24 h induction. Furthermore, nutrient limitation resulted in increased SFA and MUFA but decreased PUFA which led to reduced iodine value and increased cetane number in the present study. This indicates that two-stage model can enhance biodiesel quality from *S. costatum*.

In this study, the two-stage model enhanced both lipid productivity and biodiesel features of the diatom *S. costatum*. However, these results are based on laboratory study. If this scenario is applied in outdoor full-scale operations, cost should be considered. Compared to one-stage model, two-stage model requires an additional harvesting process that is energy-consuming. Harvesting accounts for very small proportion (< 5%) of total cost (Nagarajan et al., 2013) and meanwhile, some techniques have been developed to reduce energy consumption. For instance, dispersed air flotation can reduce energy consumption from 5.9 to 0.003 kWh/m^3 compared to traditional vacuum filtration (Coward et al., 2013). Considering that two-stage model more than doubled the lipid productivity, the cost of additional harvesting should be insignificant.

4. Conclusion

A two-stage model was used to optimize biodiesel production from the bloom-forming diatom *S. costatum* for the first time. The co-limitation of nitrogen and silicon not only increased lipid productivity but also improved biodiesel features (decreased iodine value and increased cetane number), suggesting that the two-stage model is an effective way to obtain high biodiesel production with high quality. Future investigations into other microalgae are needed to see whether this model can apply to other microalgae that have the potential for biofuel production.

Acknowledgements

This study was supported by the National Key R&D Program of China (2018YFD0900703), the Lianyungang Innovative and Entrepreneurial Doctor Program (201702), the China Postdoctoral Science Foundation (2018T110463, 2017M620270), the Six Talents Peaks in Jiangsu Province (JY-086) and Priority Academic Program Development of Jiangsu Higher Education Institutions.

Appendix A. Supplementary data

Supplementary data to this article can be found online at https://doi.org/10.1016/j.biortech.2019.121717.

References

Abu-Ghosh, S., Dubinsky, Z., Banet, G., Iluz, D., 2018. Optimizing photon dose and frequency to enhance lipid productivity of thermophilic algae for biofuel production. Bioresour. Technol. 260, 374–379.

Adeniyi, O.M., Azimov, U., Burluka, A., 2018. Algae biofuel: current status and future applications. Renewable Sustainable Energy Rev. 90, 316–335.

Aléman-Nava, G.S., Muylaert, K., Bermudez, S.P.C., Depraetere, O., Rittmann, B., Parra-Saldívar, R., Vandamme, D., 2017. Two-stage cultivation of *Nannochloropsis oculata* for lipid production using reversible alkaline flocculation. Bioresour. Technol. 226, 18–23.

Aslam, A., Thomas-Hall, S.R., Manzoor, M., Jabeen, F., Iqbal, M., Uz Zaman, Q., Schenk, P.M., Tahir, M.A., 2018. Mixed microalgae consortia growth under higher concentration of CO_2 from unfiltered coal fired flue gas: fatty acid profiling and biodiesel production. J. Photochem. Photobiol. B 179, 126–133.

Bondoc, K.G.V., Heuschele, J., Gillard, J., Vyverman, W., Pohnert, G., 2016. Selective silicate-directed motility in diatoms. Nat. Commun. 7, 10540.

Bradford, M.M., 1976. A rapid and sensitive method for the quantitation of microgram quantities of protein utilizing the principle of protein-dye binding. Anal. Biochem. 72, 248–254.

Brennan, L., Owende, P., 2010. Biofuels from microalgae-a review of technologies for production, processing, and extractions of biofuels and co-products. Renewable Sustainable Energy Rev. 14 (2), 557–577.

Chandra, R., Iqbal, H.M., Vishal, G., Lee, H.S., Nagra, S., 2019. Algal biorefinery: a sustainable approach to valorize algal-based biomass towards multiple product recovery. Bioresour. Technol. 278, 346–359.

Cho, K., Lee, C.H., Ko, K., Lee, Y.J., Kim, K.N., Kim, M.K., Chung, Y.H., Kim, D., Yeo, I.K., Oda, T., 2016. Use of phenol-induced oxidative stress acclimation to stimulate cell growth and biodiesel production by the oceanic microalga *Dunaliella salina*. Algal Res. 17, 61–66.

Coward, T., Lee, J.G., Caldwell, G.S., 2013. Development of a foam flotation system for harvesting microalgae biomass. Algal Res. 2, 135–144.

Deriaz, R.E., 1961. Routine analysis of carbohydrates and lignin in herbage. J. Sci. Food Agric. 12, 152–160.

Dickinson, S., Mientus, M., Frey, D., Amini-Hajibashi, A., Ozturk, S., Shaikh, F., Sengupta, D., El-Halwagi, M.M., 2017. A review of biodiesel production from microalgae. Clean Technol. Environ. 19 (3), 637–668.

Doan, T.T.Y., Sivaloganathan, B., Obbard, J.P., 2011. Screening of marine microalgae for biodiesel feedstock. Biomass Bioenergy 35, 2534–2544.

Fields, M.W., Hise, A., Lohman, E.J., Bell, T., Gardner, R.D., Corredor, L., Moll, K., Peyton, B.M., Gregory, W., Gerlach, R., 2014. Sources and resources: importance of nutrients, resource allocation, and ecology in microalgal cultivation for lipid accumulation. Appl. Microbiol. Biot. 98 (11), 4805–4816.

Folch, J., Lees, M., Sloane-Stantley, G.H., 1957. A simple method for the isolation and purification of total lipids from animal tissues. J. Biol. Chem. 226, 497–509.

Francisco, E.C., Neves, D.B., Jacob-Lopes, E., Franco, T.T., 2010. Microalgae as feedstock for biodiesel production: carbon dioxide sequestration, lipid production and biofuel quality. J. Chem. Technol. Biotechnol. 85 (3), 395–403.

Gao, G., Clare, A.S., Chatzidimitriou, E., Rose, C., Caldwell, G., 2018a. Effects of ocean warming and acidification, combined with nutrient enrichment, on chemical composition and functional properties of *Ulva rigida*. Food Chem. 258, 71–78.

Gao, G., Gao, K., Giordano, M., 2009. Responses to solar UV radiation of the diatom *Skeletonema costatum* (Bacillariophyceae) grown at different Zn^{2+} concentrations. J. Phycol. 45 (1), 119–129.

Gao, G., Shi, Q., Xu, Z., Xu, J., Campbell, D.A., Wu, H., 2018b. Global warming interacts with ocean acidification to alter PSII function and protection in the diatom *Thalassiosira weissflogii*. Environ. Exp. Bot. 147, 95–103.

Gao, G., Xia, J., Yu, J., Zeng, X., 2018c. Physiological response of a red tide alga (*Skeletonema costatum*) to nitrate enrichment, with special reference to inorganic carbon acquisition. Mar. Environ. Res. 133, 15–23.

Gouveia, L., Marques, A.E., Da Silva, T.L., Reis, A., 2009. *Neochloris oleabundans* UTEX# 1185: a suitable renewable lipid source for biofuel production. J. Ind. Microbiol. Biot. 36 (6), 821–826.

Griffiths, M.J., Harrison, S.T., 2009. Lipid productivity as a key characteristic for choosing algal species for biodiesel production. J. Appl. Phycol. 21 (5), 493–507.

Hildebrand, M., Davis, A.K., Smith, S.R., Traller, J.C., Abbriano, R., 2012. The place of diatoms in the biofuels industry. Biofuels 3 (2), 221–240.

IPCC, Climate Change 2013: The Physical Science Basis. Working Group I Contribution to the Fifth Assessment Report of the Intergovernmental Panel on Climate Change [T. F. Stocker, D. Qin, G-K Plattner., M. Tignor, S. K. Allen, J. Boschung, A. Nauels, Y. Xia, V. Bex, P. M. Midgley (eds.)], Cambridge Univ Press, New York, pp. 6–10.

IPCC SR1.5°C, 2018. Global Warming of 1.5 °C. An IPCC Special Report on the Impacts of Global Warming of 1.5 °C Above Pre-industrial Levels and Related Global Greenhouse Gas Emission Pathways, in the Context of Strengthening the Global Response to the Threat of Climate Change, Sustainable Development, and Efforts to Eradicate Poverty [V. Masson-Delmotte, P. Zhai, H. O. Pörtner, D. Roberts, J. Skea, P.R. Shukla, A. Pirani, W. Moufouma-Okia, C. Péan, R. Pidcock, S. Connors, J. B. R. Matthews, Y. Chen, X. Zhou, M. I. Gomis, E. Lonnoy, T. Maycock, M. Tignor, T. Waterfield (eds.)]. http://www.ipcc.ch/report/sr15/.

Jiang, X., Han, Q., Gao, X., Gao, G., 2016. Conditions optimising on the yield of biomass, total lipid, and valuable fatty acids in two strains of *Skeletonema menzelii*. Food Chem. 194, 723–732.

Knight, M.J., Senior, L., Nancolas, B., Ratcliffe, S., Curnow, P., 2016. Direct evidence of the molecular basis for biological silicon transport. Nat. Commun. 7, 11926.

Knothe, G., 2009. Improving biodiesel fuel properties by modifying fatty ester composition. Energy. Environ. Sci. 2 (7), 759–766.

Knothe, G., 2012. Fuel properties of highly polyunsaturated fatty acid methyl esters. Prediction of fuel properties of algal biodiesel. Energy Fuels 26 (8), 5265–5273.

Levitan, O., Dinamarca, J., Hochman, G., Falkowski, P.G., 2014. Diatoms: a fossil fuel of the future. Trends Biotechnol. 32 (3), 117–124.

Liu, Y., Song, X., Cao, X., Yu, Z., 2012. Responses of photosynthetic characters of *Skeletonema costatum* to different nutrient conditions. J. Plankton Res. 35 (1), 165–176.

Leynaert, A., Fardel, C., Beker, B., Soler, C., Delebecq, G., Lemercier, A., Pondaven, P., Durand, P.E., Heggarty, K., 2018. Diatom frustules nanostructure in pelagic and benthic environments. Silicon 10 (6), 2701–2709.

McNair, H.M., Brzezinski, M.A., Krause, J.W., 2018. Diatom populations in an upwelling environment decrease silica content to avoid growth limitation. Environ. Microbiol. 20 (11), 4184–4193.

Mishra, A., Medhi, K., Maheshwari, N., Srivastava, S., Thakur, I.S., 2018. Biofuel production and phycoremediation by *Chlorella* sp. ISTLA1 isolated from landfill site. Bioresour. Technol. 253, 121–129.

Moll, K.M., Gardner, R.D., Eustance, E.O., Gerlach, R., Peyton, B.M., 2014. Combining multiple nutrient stresses and bicarbonate addition to promote lipid accumulation in the diatom RGd-1. Algal Res. 5, 7–15.

Nagarajan, S., Chou, S.K., Cao, S., Wu, C., Zhou, Z., 2013. An updated comprehensive

techno-economic analysis of algae biodiesel. Bioresour. Technol. 145, 150–156.
Nayak, M., Suh, W.I., Chang, Y.K., Lee, B., 2019. Exploration of two-stage cultivation strategies using nitrogen starvation to maximize the lipid productivity in *Chlorella* sp. HS2. Bioresour. Technol. 276, 110–118.
Nelson, D.M., Tréguer, P., Brzezinski, M.A., Leynaert, A., Quéguiner, B., 1995. Production and dissolution of biogenic silica in the ocean: revised global estimates, comparison with regional data and relationship to biogenic sedimentation. Global Biogeochem. Cycl. 9, 359–372.
Pandey, A., Lee, D.J., Chang, J.S., Chisti, Y., Soccol, C.R., 2018. Biomass, Biofuels, Biochemicals: Biofuels from Algae. Elsevier.
Pereira, H., Barreira, L., Custódio, L., Alrokayan, S., Mouffouk, F., Varela, J., Abu-Salah, K., Ben-Hamadou, R., 2013. Isolation and fatty acid profile of selected microalgae strains from the Red Sea for biofuel production. Energies 6 (6), 2773–2783.
Rekha, V., Gurusamy, R., Santhanam, P., Devi, A.S., Ananth, S., 2012. Culture and biofuel production efficiency of marine microalgae *Chlorella marina* and *Skeletonema costatum*. Indian J. Geo-Mar. Sci. 41 (2), 152–158.
Rodolfi, L., Chini Zittelli, G., Bassi, N., Padovani, G., Biondi, N., Bonini, G., Tredici, M.R., 2009. Microalgae for oil: strain selection, induction of lipid synthesis and outdoor mass cultivation in a low-cost photobioreactor. Biotechnol. Bioeng. 102 (1), 100–112.
Roessler, P.G., 1988. Effects of silicon deficiency on lipid composition and metabolism in the diatom *Cyclotella cryptica*. J. Phycol. 24 (3), 394–400.
Sakarika, M., Kornaros, M., 2019. *Chlorella vulgaris* as a green biofuel factory: comparison between biodiesel, biogas and combustible biomass production. Bioresour. Technol. 273, 237–243.
Shrestha, R.P., Hildebrand, M., 2017. Development of a silicon limitation inducible expression system for recombinant protein production in the centric diatoms *Thalassiosira pseudonana* and *Cyclotella cryptica*. Microb. Cell Fact. 16 (145), 1–14.
Shuba, E.S., Kifle, D., 2018. Microalgae to biofuels: 'Promising'alternative and renewable energy, review. Renewable Sustainable Energy Rev. 81, 743–755.
Sibi, G., Shetty, V., Mokashi, K., 2016. Enhanced lipid productivity approaches in microalgae as an alternate for fossil fuels – a review. J. Energy Inst. 89 (3), 330–334.
Smith, S.R., Glé, C., Abbriano, R.M., Traller, J.C., Davis, A., Trentacoste, E., Vernet, M., Allen, A.E., Hildebrand, M., 2016. Transcript level coordination of carbon pathways during silicon starvation-induced lipid accumulation in the diatom *Thalassiosira pseudonana*. New Phytol. 210 (3), 890–904.
Souffreau, C., Vanormelingen, P., Verleyen, E., Sabbe, K., Vyverman, W., 2010. Tolerance of benthic diatoms from temperate aquatic and terrestrial habitats to experimental desiccation and temperature stress. Phycologia 49, 309–324.
Yang, Z.K., Niu, Y.F., Ma, Y.H., Xue, J., Zhang, M.H., Yang, W.D., Liu, J.S., Lu, S.H., Guan, Y., Li, H.Y., 2013. Molecular and cellular mechanisms of neutral lipid accumulation in diatom following nitrogen deprivation. Biotechnol. Biofuels 6 (67), 1–14.
Yuan, W., Gao, G., Shi, Q., Xu, Z., Wu, H., 2018. Combined effects of ocean acidification and warming on physiological response of the diatom *Thalassiosira pseudonana* to light challenges. Mar. Environ. Res. 135, 63–69.